(14) TI- ALEX(01)-TR-77-07

(6) EXTRACTION OF LONG-PERIOD BODYWAVES, (12)

(9) TECHNICAL REPORT NO. 7

VELA NETWORK EVALUATION AND AUTOMATIC PROCESSING RESEARCH

Prepared by

(10) Stephen S. Lane

TEXAS INSTRUMENTS INCORPORATED
Equipment Group
Post Office Box 6015
Dallas, Texas 75222

Prepared for

AIR FORCE TECHNICAL APPLICATIONS CENTER
Alexandria, Virginia 22314

Sponsored by

ADVANCED RESEARCH PROJECTS AGENCY
Nuclear Monitoring Research Office
ARPA Program Code No. 7F10
ARPA Order No. 2551

A038 290

(11) 14 November 1977 (12) 37 p.

Acknowledgment: This research was supported by the Advanced Research Projects Agency, Nuclear Monitoring Research Office, under Project VELA-UNIFORM, and accomplished under the technical direction of the Air Force Technical Applications Center under Contract Number F08606-77-C-0004,

(8) ARPA Order-2551

405 076

ALEX(01)-TR-77-07

12

EXTRACTION OF LONG-PERIOD BODYWAVES

TECHNICAL REPORT NO.7

VELA NETWORK EVALUATION AND AUTOMATIC PROCESSING RESEARCH

Prepared by
Stephen S. Lane

TEXAS INSTRUMENTS INCORPORATED
Equipment Group
Post Office Box 6015
Dallas, Texas 75222

Prepared for

AIR FORCE TECHNICAL APPLICATIONS CENTER
Alexandria, Virginia 22314

Sponsored by

ADVANCED RESEARCH PROJECTS AGENCY
Nuclear Monitoring Research Office
ARPA Program Code No. 7F10
ARPA Order No. 2551

14 November 1977

Acknowledgment: This research was supported by the Advanced Research Projects Agency, Nuclear Monitoring Research Office, under Project VELA-UNIFORM, and accomplished under the technical direction of the Air Force Technical Applications Center under Contract Number F08606-77-C-0004.

UNCLASSIFIED

AD50318

SECURITY CLASSIFICATION OF THIS PAGE (When Data Entered)

REPORT DOCUMENTATION PAGE	READ INSTRUCTIONS BEFORE COMPLETING FORM
1. REPORT NUMBER	2. GOVT ACCESSION NO. / 3. RECIPIENT'S CATALOG NUMBER
4. TITLE (and Subtitle): EXTRACTION OF LONG-PERIOD BODYWAVES	5. TYPE OF REPORT & PERIOD COVERED: Technical
	6. PERFORMING ORG. REPORT NUMBER: ALEX(01)-TR-77-07
7. AUTHOR(s): (10) Stephen S. Lane	8. CONTRACT OR GRANT NUMBER(s): (15) F08606-77-C-0004
9. PERFORMING ORGANIZATION NAME AND ADDRESS: Texas Instruments Incorporated, Equipment Group, Dallas, Texas 75222	10. PROGRAM ELEMENT, PROJECT, TASK AREA & WORK UNIT NUMBERS: VELA T/7705/B/ETR
11. CONTROLLING OFFICE NAME AND ADDRESS: Advanced Research Projects Agency, 1400 Wilson Boulevard, Arlington, Virginia 22209	12. REPORT DATE: 14 November 1977
	13. NUMBER OF PAGES: 36
14. MONITORING AGENCY NAME & ADDRESS (if different from Controlling Office): Air Force Technical Applications Center, VELA Seismological Center, Alexandria, Virginia 22314	15. SECURITY CLASS. (of this report): UNCLASSIFIED
	15a. DECLASSIFICATION/DOWNGRADING SCHEDULE

16. DISTRIBUTION STATEMENT (of this Report)

APPROVED FOR PUBLIC RELEASE, DISTRIBUTION UNLIMITED

17. DISTRIBUTION STATEMENT (of the abstract entered in Block 20, if different from Report)

18. SUPPLEMENTARY NOTES

ARPA Order No. 2551

19. KEY WORDS (Continue on reverse side if necessary and identify by block number)

Seismology
Long-Period Bodywaves
Polarization Filter
Radiation Pattern
Detection Threshold

20. ABSTRACT (Continue on reverse side if necessary and identify by block number)

A polarization filter for long-period bodywaves was developed and tested on 100 events from the Kurile Islands and measured at the Guam Seismic Research Observatory. Fifty percent detection thresholds before processing were m_b = 5.5 and 5.1 for P and S waves, respectively, and were unchanged by the filter unless a substantial false alarm rate was allowed, when the P threshold was reduced to m_b = 5.0. There is evidence that this poor performance is due to the data set used.

DD FORM 1 JAN 73 1473 EDITION OF 1 NOV 65 IS OBSOLETE

UNCLASSIFIED

SECURITY CLASSIFICATION OF THIS PAGE (When Data Entered)

ABSTRACT

A polarization filter for long-period bodywaves was developed and tested on 100 events from the Kurile Islands and measured at the Guam Seismic Research Observatory. Fifty percent detection thresholds before processing were m_b = 5.5 and 5.1 for P and S waves, respectively, and were unchanged by the filter unless a substantial false alarm rate was allowed, when the P threshold was reduced to m_b = 5.0. There is evidence that this poor performance is due to the data set used.

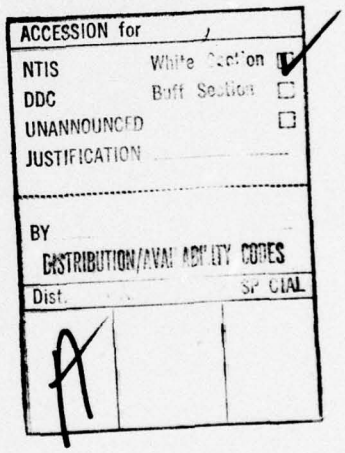

TABLE OF CONTENTS

SECTION	TITLE	PAGE
	ABSTRACT	iii
	ACKNOWLEDGMENTS	iv
I.	INTRODUCTION	I-1
II.	PROCESSORS	II-1
III.	DATA SET	III-1
IV.	RESULTS	IV-1
	A. DETECTION THRESHOLDS	IV-1
	B. MAGNITUDES	IV-9
V.	CONCLUSIONS	V-1
VI.	REFERENCES	VI-1

LIST OF FIGURES

FIGURE	TITLE	PAGE
II-1	ILPA VERTICAL P AND S WAVES	II-2
II-2	EXPECTED ($\hat{K}$) AND OBSERVED ($\hat{P}$) PROPAGATION VECTORS	II-5
II-3	WEIGHTS FOR ADAPTIVE FILTER AS A FUNCTION OF θ	II-6
II-4	SEISMOGRAMS FROM m_b = 5.7 EVENT	II-8
II-5	SEISMOGRAMS FROM m_b = 4.6 EVENT	II-9
III-1	DISTRIBUTION OF EVENT SAMPLES	III-2
IV-1	P WAVE BANDPASS FILTERED DETECTIONS	IV-2
IV-2	S WAVE BANDPASS FILTERED DETECTIONS	IV-3
IV-3	P WAVE ADAPTIVE FILTER DETECTIONS	IV-5
IV-4	S WAVE ADAPTIVE FILTER DETECTIONS	IV-6
IV-5	P WAVE ADAPTIVE FILTER DETECTIONS WITH LIBERAL DETECTION CRITERIA	IV-7
IV-6	S WAVE ADAPTIVE FILTER DETECTIONS WITH LIBERAL DETECTION CRITERIA	IV-8
IV-7	EPICENTERS FOR P WAVE DETECTIONS	IV-10
IV-8	M_B VERSUS m_b FOR P WAVES	IV-12
IV-9	EPICENTERS FOR S WAVE DETECTIONS	IV-13
IV-10	M_B VERSUS m_b FOR S WAVES	IV-14

SECTION I
INTRODUCTION

This report presents the results of a study of detectors for long-period bodywave phases. It was motivated by the fact that there is a good separation between the earthquake and explosion populations by means of long-period bodywave magnitudes (Kisslinger et al., 1974), and these phases therefore provide additional discriminatory power where they can be detected.

When a simple bandpass filter is used as the only processing scheme the 50% detection threshold, the short-period magnitude at which half of all events are detected by means of long-period bodywaves, is about m_b = 5.5 for P waves and about 5.1 for S waves, considerably higher than the corresponding threshold for surface waves of about m_b = 4.6 (Strauss, 1977).

The processors described in this report take advantage of the polarization of P and S waves. Test events show good improvement in signal-to-noise ratio, but when evaluated on a data set consisting of earthquakes in the Kurile Islands recorded at the Guam Seismic Research Observatory, no reduction in threshold was achieved. There is evidence that this is due to the particular data set used, and that the P detection threshold may be as low as m_b = 5.0.

In Section II the processing schemes used here are described, and examples of their effects on data presented. Section III describes the data sample investigated, and Section IV gives detection thresholds and long-period bodywave magnitudes found here. Section V presents conclusions and recommendations.

SECTION II
PROCESSORS

A natural first step in the extraction of long-period bodywaves from seismic noise is to form beams at the appropriate velocity at arrays such as the Iranian Long Period Array (ILPA) and the reconfigured ALPA array in Alaska. This approach was discarded for the following reasons.

Since ILPA and the reconfigured ALPA are only seven-element arrays, the maximum noise suppression to be found there assuming uncorrelated noise is about 8 dB. Strauss (1976) has found signal-to-noise ratio improvements on the order of 3 to 6 dB there, consistent with the expected suppression of uncorrelated noise and some signal degradation. His results apply to surface waves propagating at 3.6 km/sec. In the present study beams on a few large events at the appropriate bodywave phase velocity of 12.5 km/sec did not yield even those reduced gains. This may be attributed to two causes.

First, visual examination of individual site records indicates that site-to-site similarity is not very good for long-period bodywaves. Such records are presented in Figure II-1 for an event from the Greece-Albanian border. Considerable signal amplitude degradation may be expected in beams from such an event.

Second, the lack of similarity displayed in Figure II-1 suggests that beams at P and S velocities will not only degrade amplitudes but waveforms, in the sense that the plane and linear polarization of these phases will be contaminated by beamforming. Since previous experience with signal processors has suggested that adaptive filters searching for constants of the motion are highly effective (Lane, 1976), it was decided to use data in which signals were best preserved.

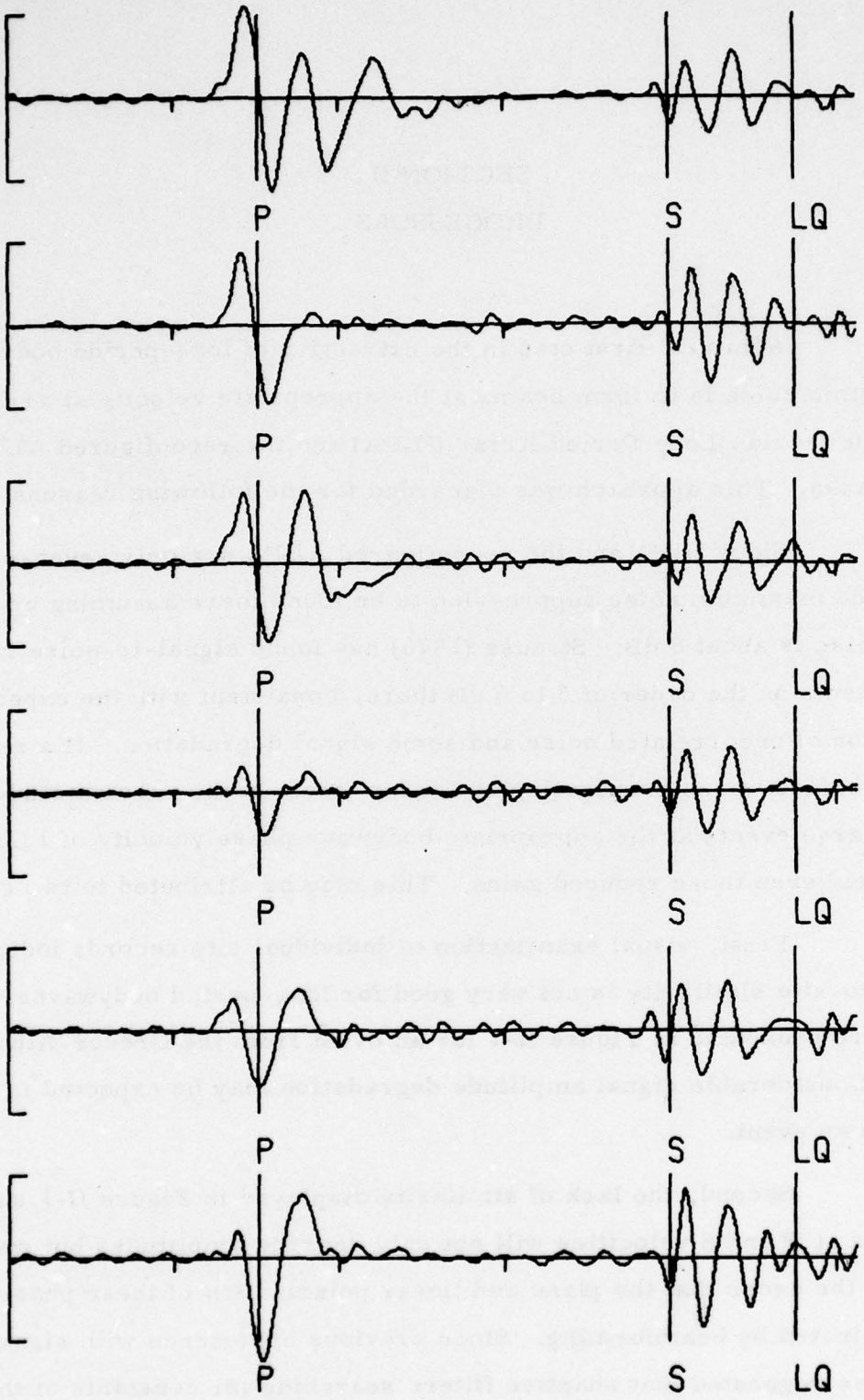

FIGURE II-1

ILPA VERTICAL P AND S WAVES

Long-period data recorded at the Seismic Research Observatories (SRO) were chosen for this purpose. These results will then be applicable to this increasingly important type of data, and can be extrapolated to beam data if beams which preserve signal similarity can be found.

Since adaptive filters are non-linear due to their dependence on the data, it is important that they be preceded by the best possible prefilter. This will be in general a Wiener filter, using as a reference spectrum one from a typical event from the region of interest, or an average over such spectra. However, examination of the few large events from the Kurile Islands, the region used in this study, showed that bodywaves from there show as much variation between one another as they do from site to site as shown in Figure II-1. An average of such signals would probably not be representative of the Kurile Island earthquake population. Consequently, a simple bandpass filter, rejecting all energy outside the frequency range 0.024-0.059 Hz, was used as the prefilter in this study.

The adaptive filters used here searched for linearly polarized motion in the correct emergence direction for extracting P waves and plane polarized motion perpendicular to the emergence direction to find S waves. Following the form of the three component adaptive filter developed for surface waves (Lane, 1976), each filter segments the vertical, radial, and transverse motion, Fourier transforms each segment, applies a filter whose weights in the frequency domain depended on the behavior of the total motion, inverse transforms, and smooths together overlapping segments to produce a continuous output waveform.

Variations in the design of such filters lie in the way the filter weights depend on the data. In the present case two approaches were tried. First, each Fourier coefficient within the frequency interval where the signal energy was expected was tested separately for the correct polarization, and an independent weight was assigned to real and imaginary coefficients.

Because such a filter is not zero phase, and disperses the signal, it was rejected during preliminary testing in favor of an approach where the weights were determined from and applied to the total Fourier amplitude.

To search for linearly polarized motion, a spatial propagation vector $\hat{P}$ was formed at each frequency as shown in Figure II-2. Its amplitude along each axis was the square root of the sum of the squares of imaginary and real Fourier coefficients of the motion along that axis, suitably normalized so that the vector's amplitude was unity. The scalar product between this vector and a unit vector $\hat{K}$ in the expected propagation direction, as determined by the epicentral distance, equals the cosine of the angle θ between the apparent propagation direction of energy at that frequency and the propagation direction for P waves from the region of interest. In general P will not lie in the vertical-radial plane, due to contamination of the signal with noise.

If θ is small, the energy may be attributed to a P wave, whereas if it is near 90°, it might be an S wave which have nearly identical emergence directions to P waves. Filter weights for extraction of either P or S waves can then be assigned using the same angle as a criterion. Choosing the way in which to do this is the remaining part of the filter design.

A Monte Carlo method was used to find the probability distribution function of the angle between the true and apparent propagation directions, assuming a model with a P wave in the true propagation direction, and additive uncorrelated noise. This procedure has been discussed more fully in Lane (1976). The probability distribution found for narrowband signal-to-noise ratios near 2.0 may be roughly approximated by the curve of Figure II-3, which was chosen for the filter weighting function. At higher signal-to-noise ratios the probability distribution function peaks more sharply near zero degrees, while at low signal-to-noise ratios is becomes flat. The probability distribution function is of course normalized to unit area, while the filter weights of Figure II-3 are chosen to be one at angles less than 20 degrees.

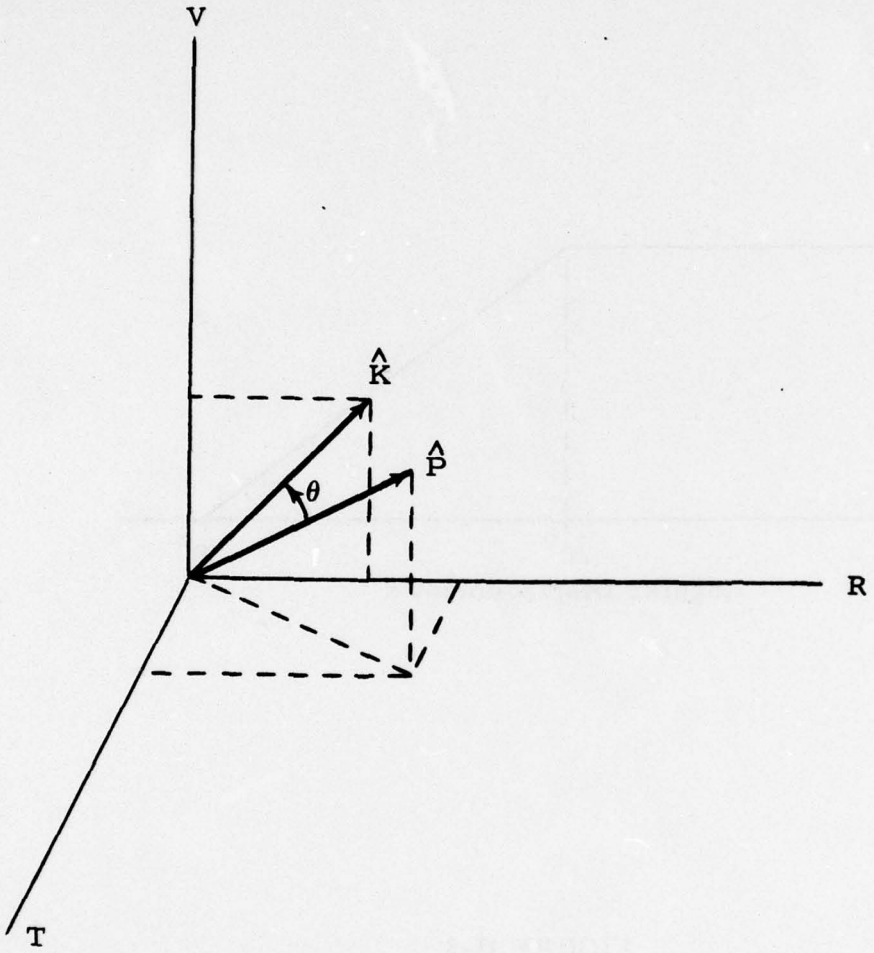

FIGURE II-2
EXPECTED ($\hat{K}$) AND OBSERVED ($\hat{P}$) PROPAGATION VECTORS

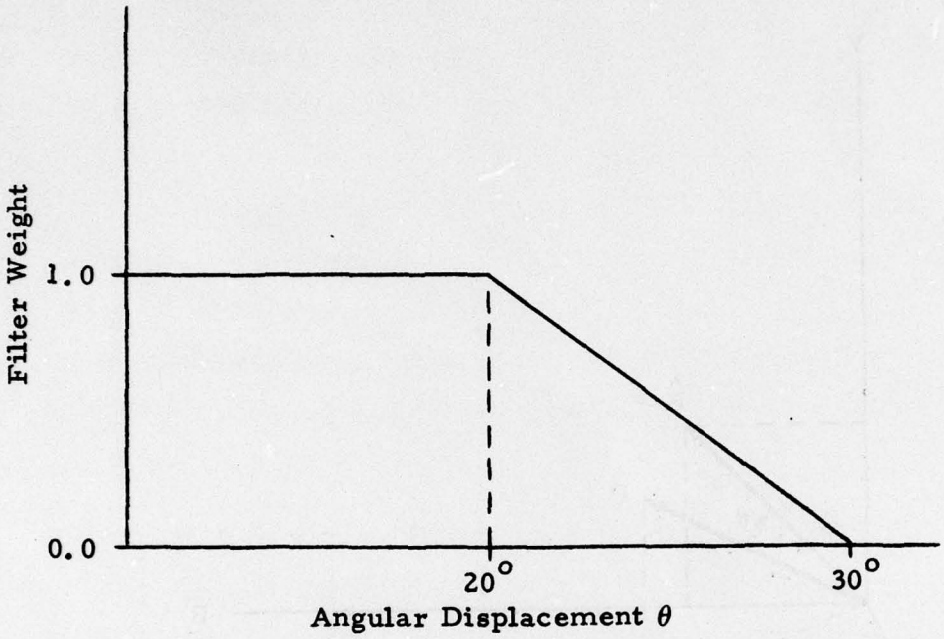

FIGURE II-3

WEIGHTS FOR ADAPTIVE FILTER
AS A FUNCTION OF θ

The same filter weights were chosen for the S wave filter, except that in that case the angle plotted on the ordinate of Figure II-3 refers to the angular distance of the particle motion vector from a plane perpendicular to the propagation vector, i.e., $\pi/2-\theta$. Thus, both SH and SV waves will be passed by this filter.

Only the vertical and radial traces are displayed for the output of the P wave filter, since no motion is expected on the transverse component. All three components of the S wave filter are displayed, since in general both SV and SH waves are possible. Such an output for a large event, for which P and S phases were detected on the bandpass filtered traces, is shown in Figure II-4. The P wave filter traces do not extend past the S wave arrival time, since S motion often passed through the P wave filter and dominated the trace. The complementary effect can be seen on the S wave traces in Figure II-4 between the P and S phase arrival times, where there are large deflections presumably due to P motion leaking through the S filter. A smaller event is shown in Figure II-5, and was detected on both P and S filters. Considerable noise precedes this event.

Leakage of compressional wave energy through the sheer wave filter, to appear as motion between the P and S arrival times on the S wave detector, implies that the models used here do not fit the data particularly well. This is true for both large and small events, where it is a more serious problem, since it suggests that the design of each detector could be improved. Such improvement should be part of any further study of this problem.

Noise suppression for the event in Figure II-4 was complete, in that the RMS noise amplitude before the signal arrival was zero. The noise suppression by the S wave filter ranged between 25 and 35 dB. For the event in Figure II-5, noise suppression was much less, as were starting noise amplitudes. The P wave filter suppressed the noise by 10 to 15 dB, while the suppression by the S wave filter ranged from 5 to 15 dB. These figures imply

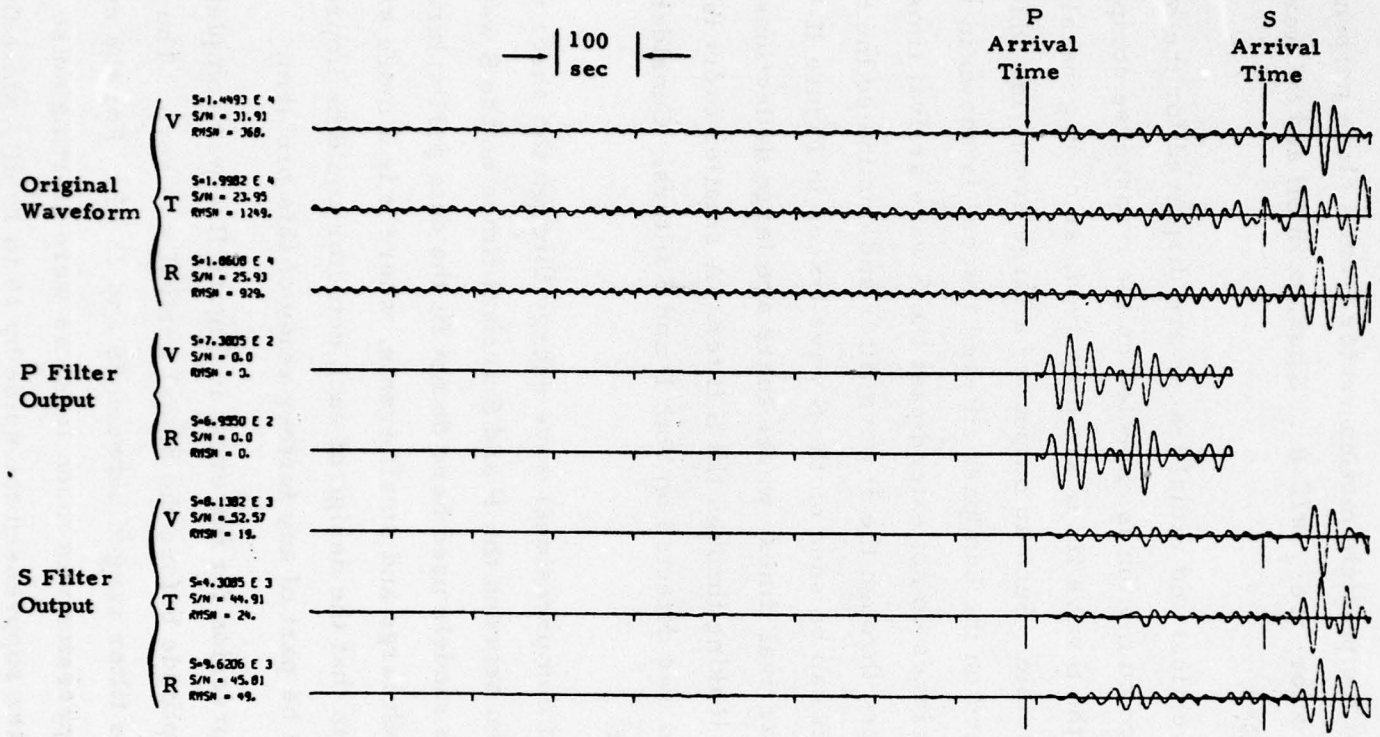

FIGURE II-4

SEISMOGRAMS FROM m_b = 5.7 EVENT

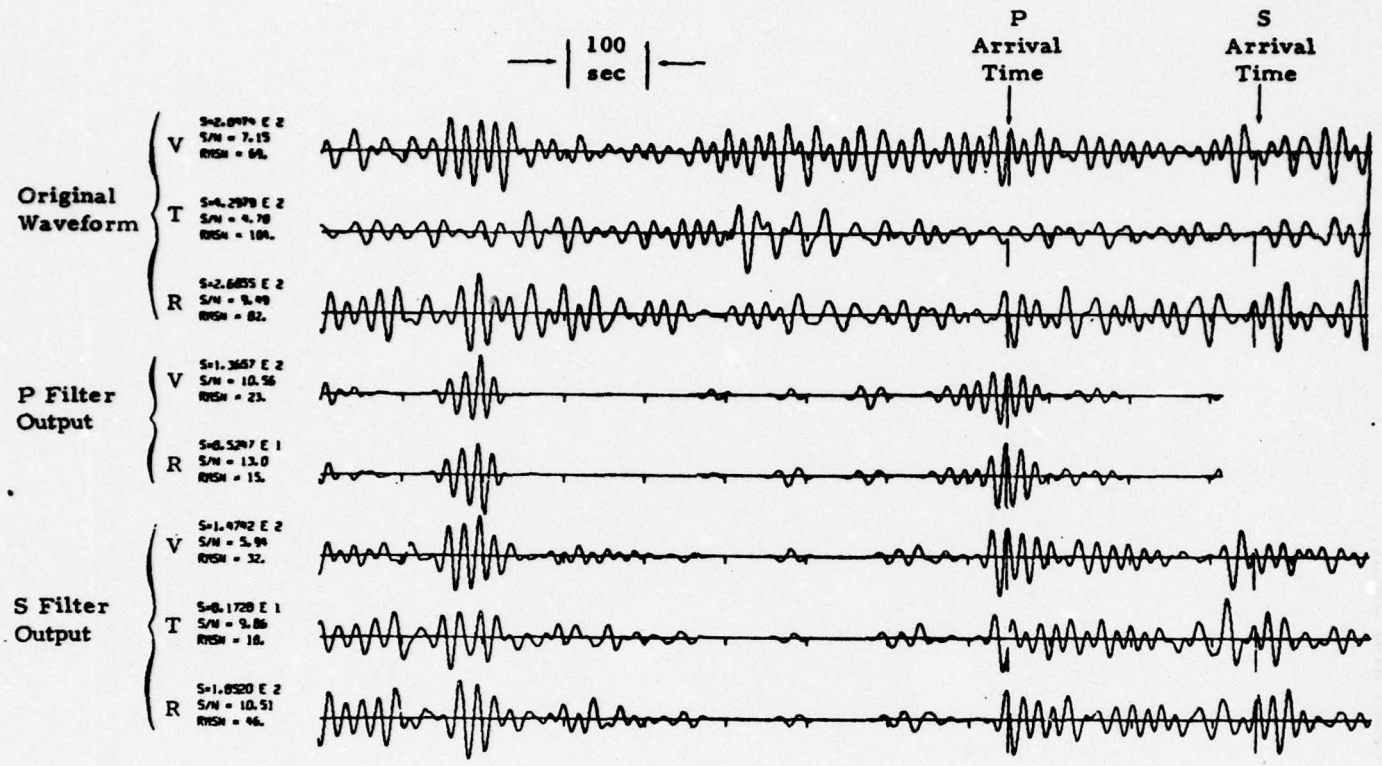

FIGURE II-5

SEISMOGRAMS FROM m_b = 4.6 EVENT

gains from 0.2 to 0.7 magnitude units if signals are passed unchanged. Signal degradation amounts to about 5 dB, however, presumably caused again by lack of agreement between model and data.

SECTION III
DATA SET

Since the most convincing test of a detector is to evaluate its performance directly on a large suite of events, that procedure was used in this study. All earthquakes reported by NORSAR between 1 January 1976 and 27 June 1976 in the Kurile Islands region were examined with the detector described in Section II. NORSAR m_b's were used throughout this study. It was hoped that the combination of constant event location and recording station would remove the effect of those variables from the evaluation of the detector's reduction in detection threshold.

Guam is 32° distant from the Kurile Islands, which form an active seismic region. This distance is a reasonable one at which to search for bodywaves in that the P and S phases are well separated in arrival times, and yet may still have reasonably large amplitudes. A total of 114 events were available, ranging in short-period bodywave magnitude from 3.3 to 5.7.

Some large events in this set were found to be part of an earthquake swarm, and consequently the root-mean-square noise levels at the predicted P and S wave arrival times for most of these events were as high as 800 μm, roughly 50 times the average value when no swarm was taking place. Since the model developed by Ringdal (1974) and used here for estimating detection thresholds assumes a Gaussian distribution of noise magnitudes, those events arriving in a background of systematically rather than randomly varying noise cannot be legitimately used for threshold estimation. Accordingly, events with noise amplitudes preceding the signal arrival of more than 100 μm were eliminated from the data set, leaving a total of 100 events. Their distribution is shown in Figure III-1.

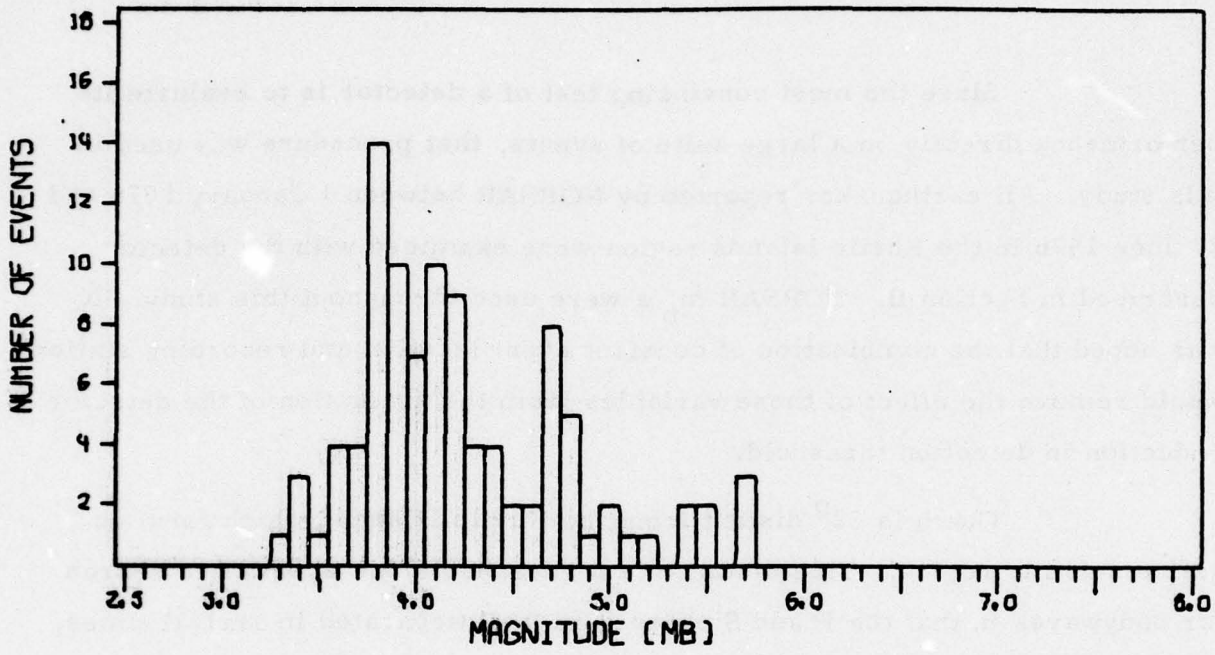

FIGURE III-1

DISTRIBUTION OF EVENT SAMPLES

SECTION IV
RESULTS

All 100 events were examined on the bandpass filtered traces for P or S detections. Detection was allowed if the peak motion occurred within 40 seconds of the predicted arrival time, and that peak was twice as large as any peak in the preceding 600 seconds of the record. Detections claimed for bodywaves will not be as reliable as those for surface waves, however, due to the lack of dispersion in bodywaves, an important requirement for detection of surface waves.

A. DETECTION THRESHOLDS

Detection histograms and best fits of Ringdal's (1975) constant plus cumulative Gaussian distribution to the associated detection probabilities are shown for the bandpass filtered traces in Figures IV-1 and IV-2 for P and S phases, respectively. The data for P waves is so sparse that it can only be claimed that the 50% detection threshold is high. The data fit the model much better for S detections, where the 50% detection threshold is $m_b = 5.1$.

Next, all 100 events were processed with the standard filter weights, and detections claimed using the criteria listed above, with one modification. The interval between the P and S arrival times on the S wave traces were disregarded when requiring that the S motion be twice the amplitude of a peak in the preceding noise gate, and the same noise gate was used for P and S detections. This eliminated the possibility that valid S detections might be rejected due to leakage of P waves through the S detector noise gate, as occurred for the large event of Figure II-3.

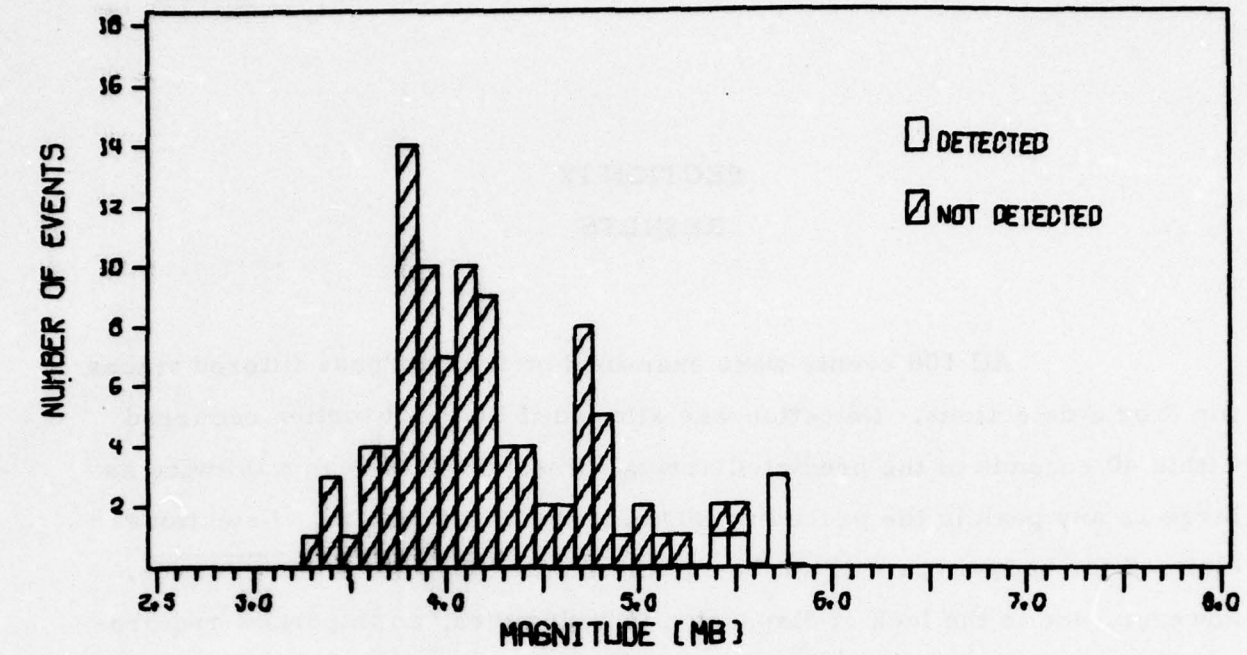

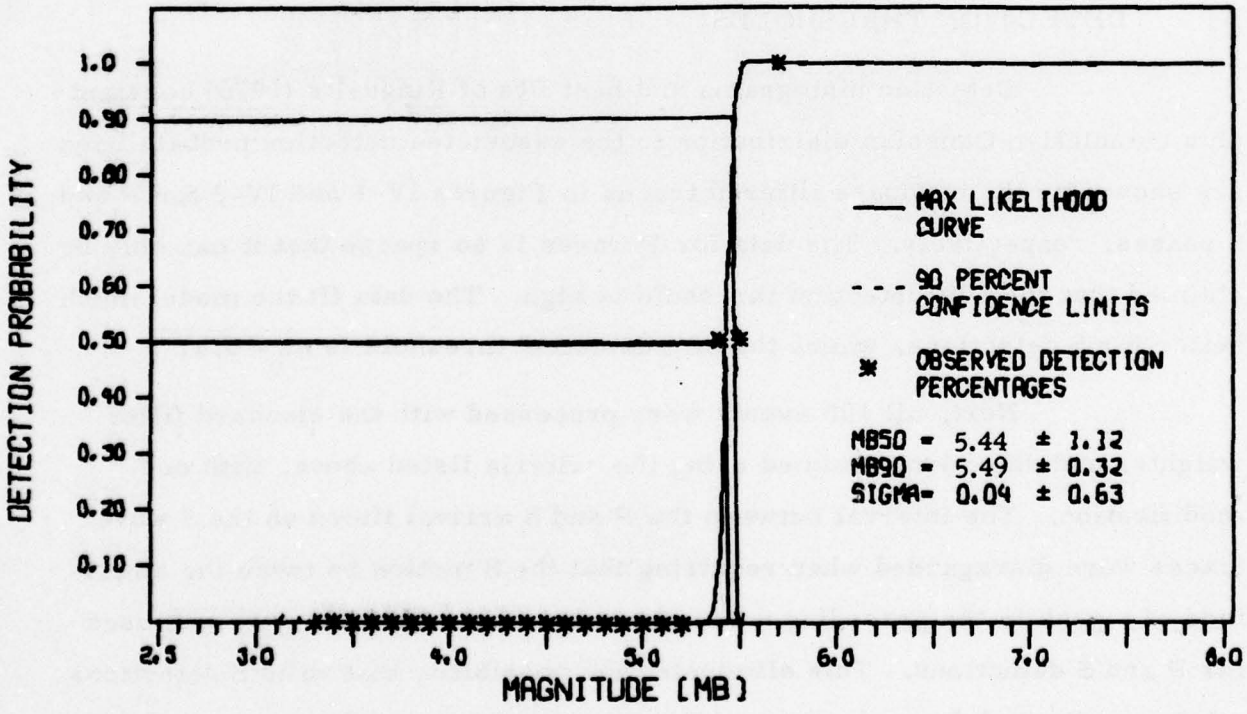

FIGURE IV-1

P WAVE BANDPASS FILTERED DETECTIONS

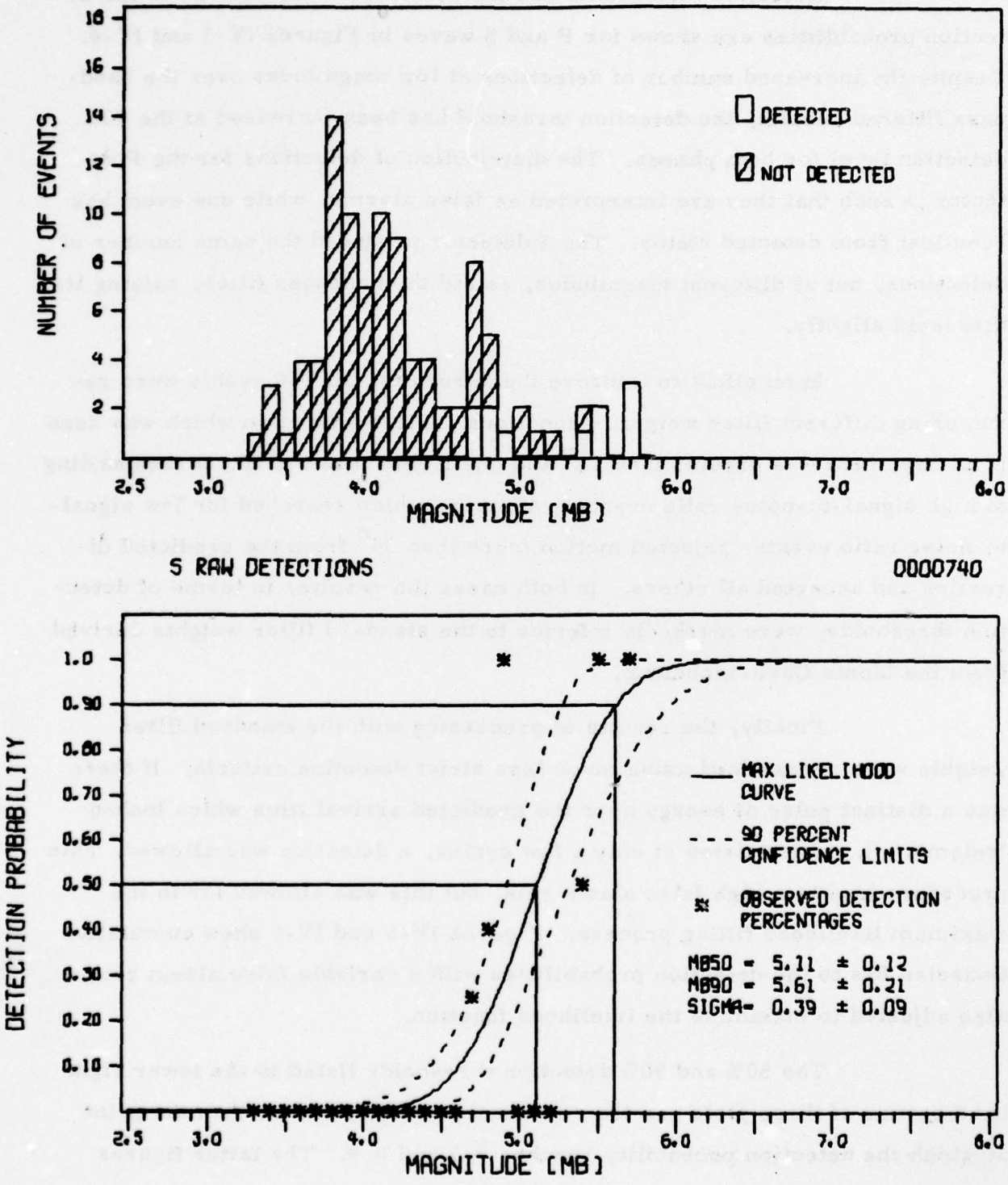

FIGURE IV-2

S WAVE BANDPASS FILTERED DETECTIONS

Detection histograms and the maximum likelihood fit to the detection probabilities are shown for P and S waves in Figures IV-3 and IV-4. Despite the increased number of detections at low magnitudes over the bandpass filtered results, the detection threshold has been increased at the 90% detection level for both phases. The distribution of detections for the P detector is such that they are interpreted as false alarms, while one event has been lost from detected status. The S detector produced the same number of detections, but at different magnitudes, as did the bandpass filter, raising its threshold slightly.

In an effort to improve these results, all 100 events were rerun using different filter weighting functions. First a function which was zero if its argument was greater than 18° and one if less was tested, corresponding to high signal-to-noise ratio events. Another, which searched for low signal-to-noise ratio events, rejected motion more than 35° from the predicted direction and accepted all others. In both cases the results, in terms of detection thresholds, were markedly inferior to the standard filter weights derived from the Monte Carlo technique.

Finally, the results of processing with the standard filter weights were reexamined using much less strict detection criteria. If there was a distinct pulse of energy near the predicted arrival time which looked 'seismic', i.e., consisted of only a few cycles, a detection was allowed. This procedure lead to a high false alarm rate, but this was allowed for in the maximum likelihood fitting process. Figures IV-5 and IV-6 show cumulative Gaussian fits to the detection probabilities with a variable false alarm rate, also adjusted to maximize the likelihood function.

The 50% and 90% detection thresholds listed in the lower right hand corner of these plots are the correct thresholds, rather than the point at which the detection probability reaches 0.5 and 0.9. The latter figures include the contribution of false alarms, whereas the former are parameters in the fit to true detections.

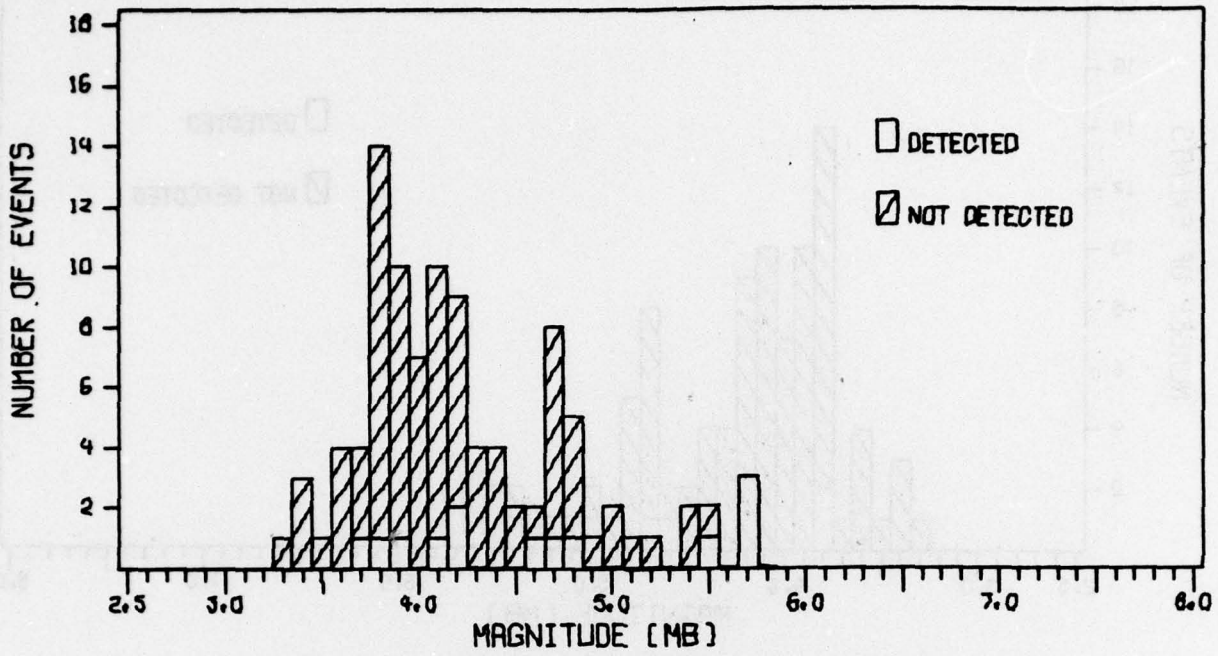

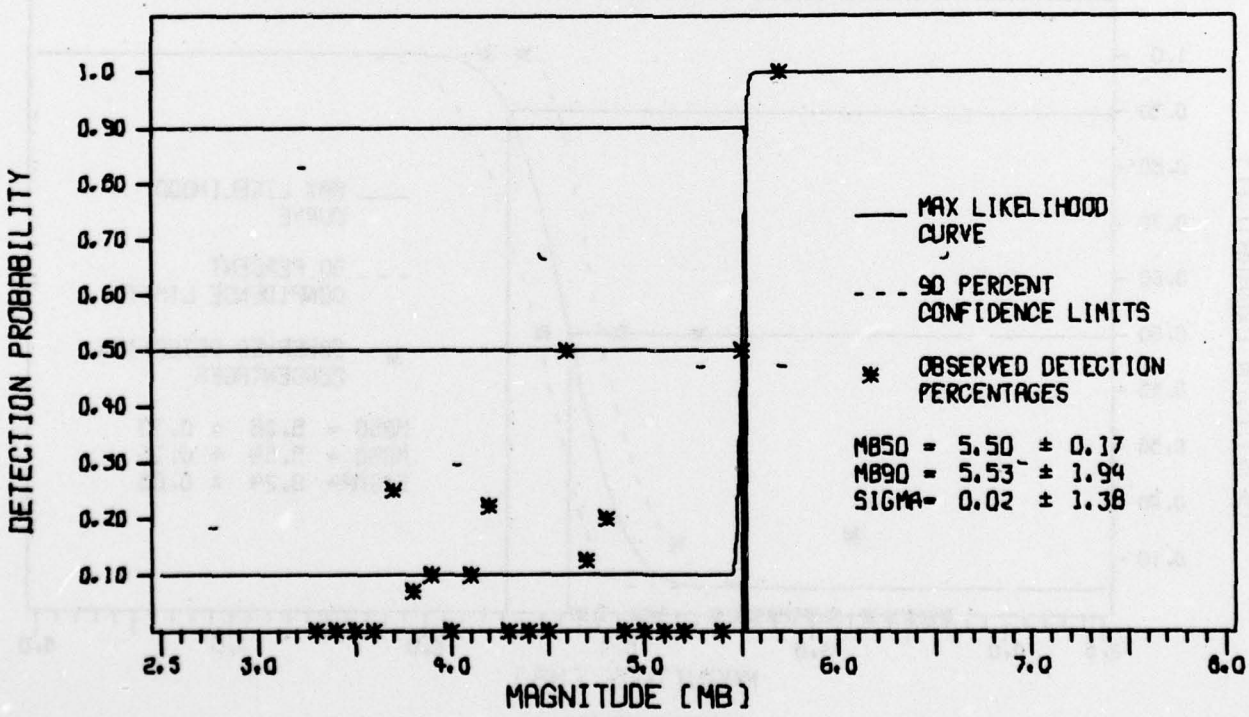

FIGURE IV-3

P WAVE ADAPTIVE FILTER DETECTIONS

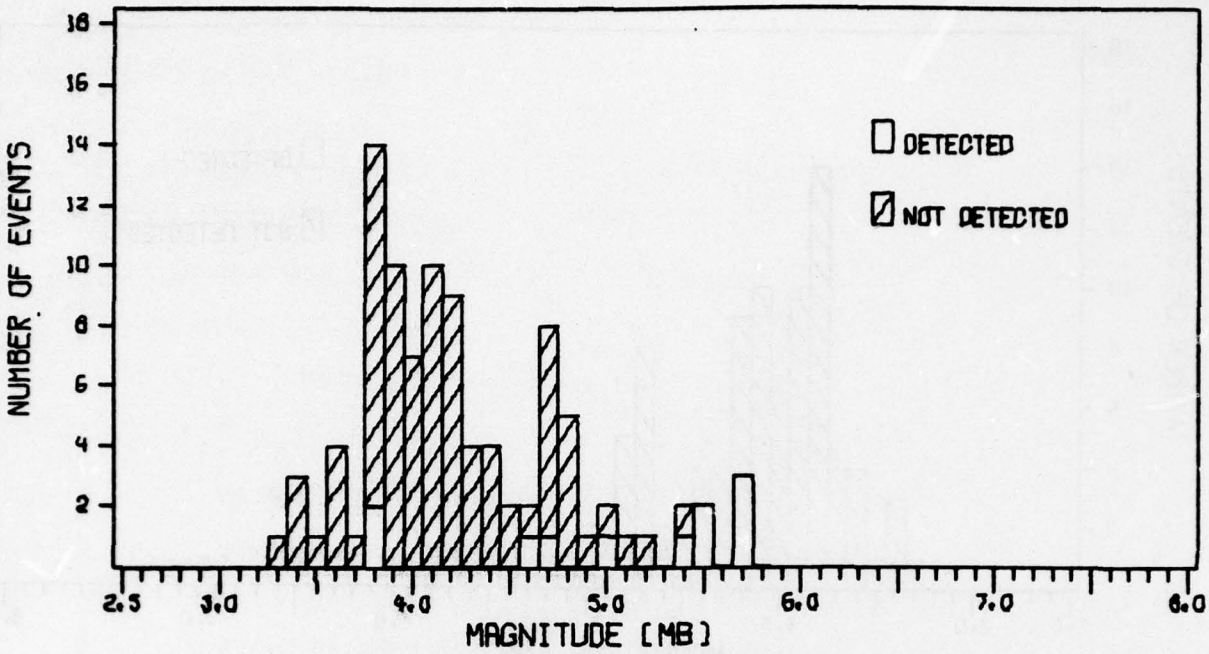

20-30 DEGREE S DETECTIONS BEST RESULTS

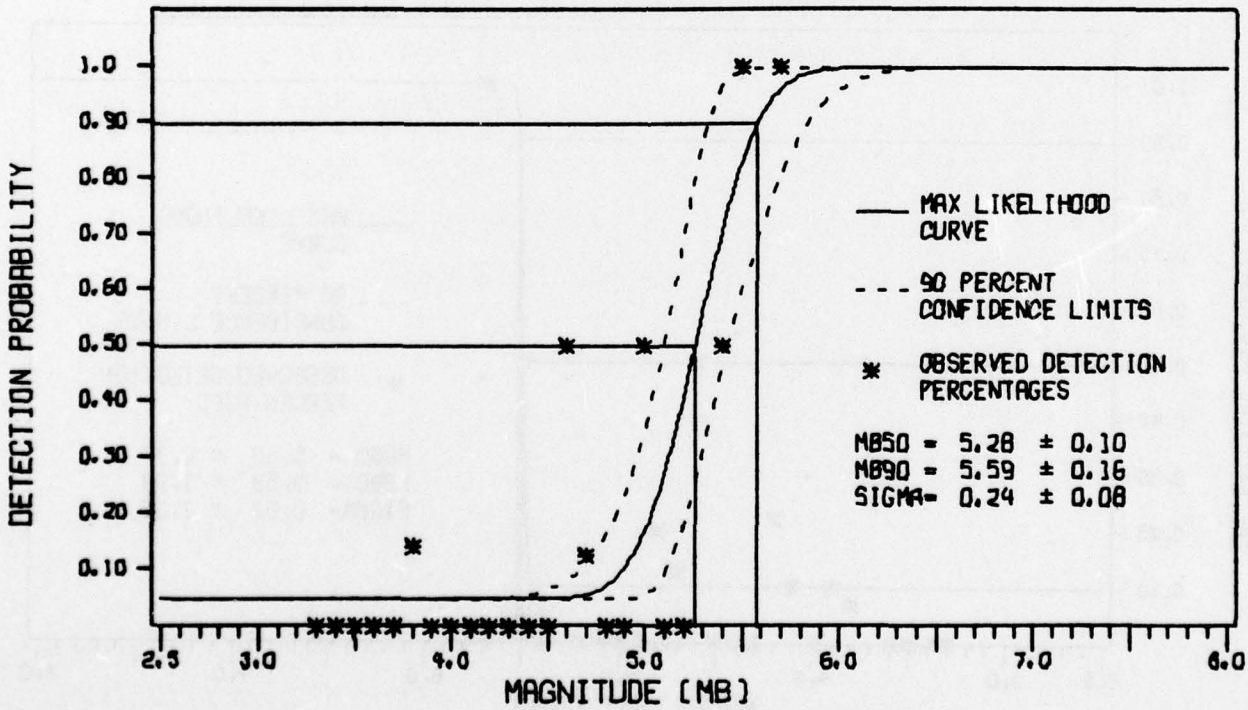

FIGURE IV-4

S WAVE ADAPTIVE FILTER DETECTIONS

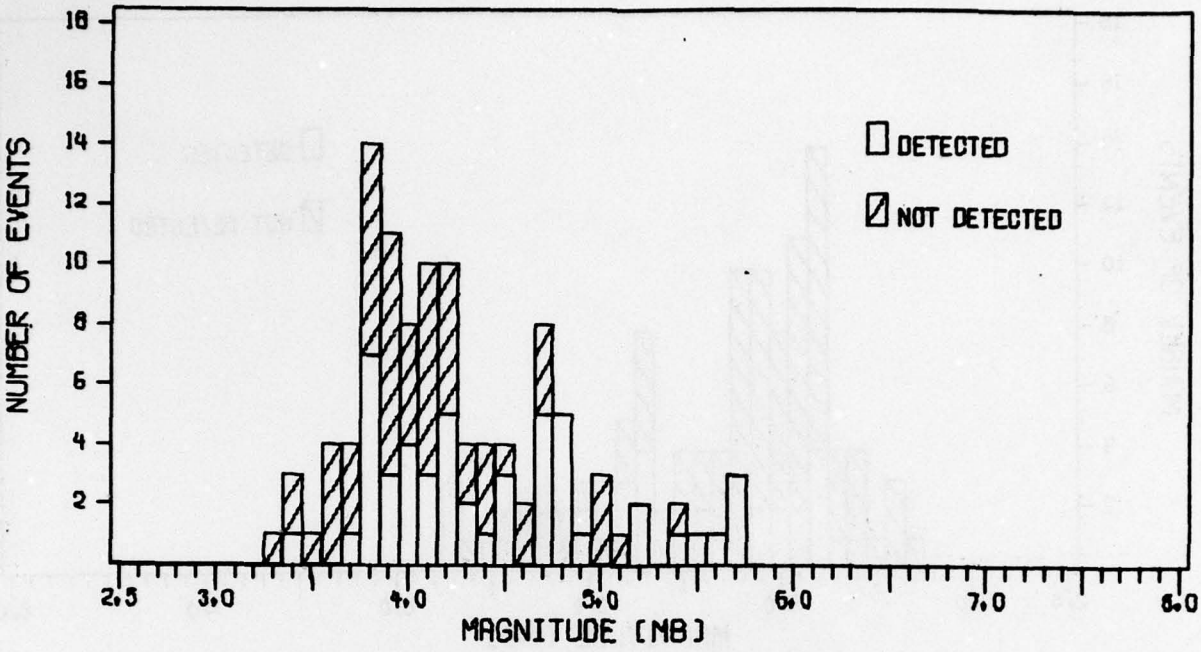

LIBERAL CRITERIA FOR 20-30 P DETECTOR

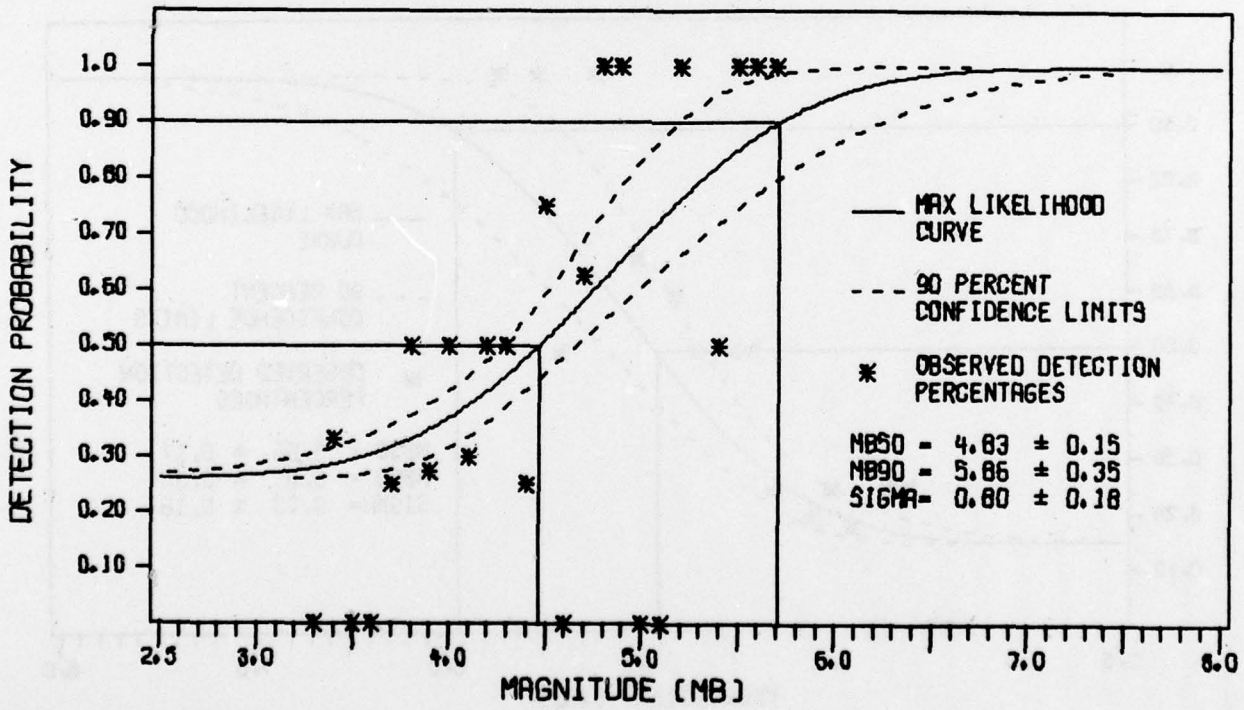

FIGURE IV-5

P WAVE ADAPTIVE FILTER DETECTIONS WITH LIBERAL DETECTION CRITERIA

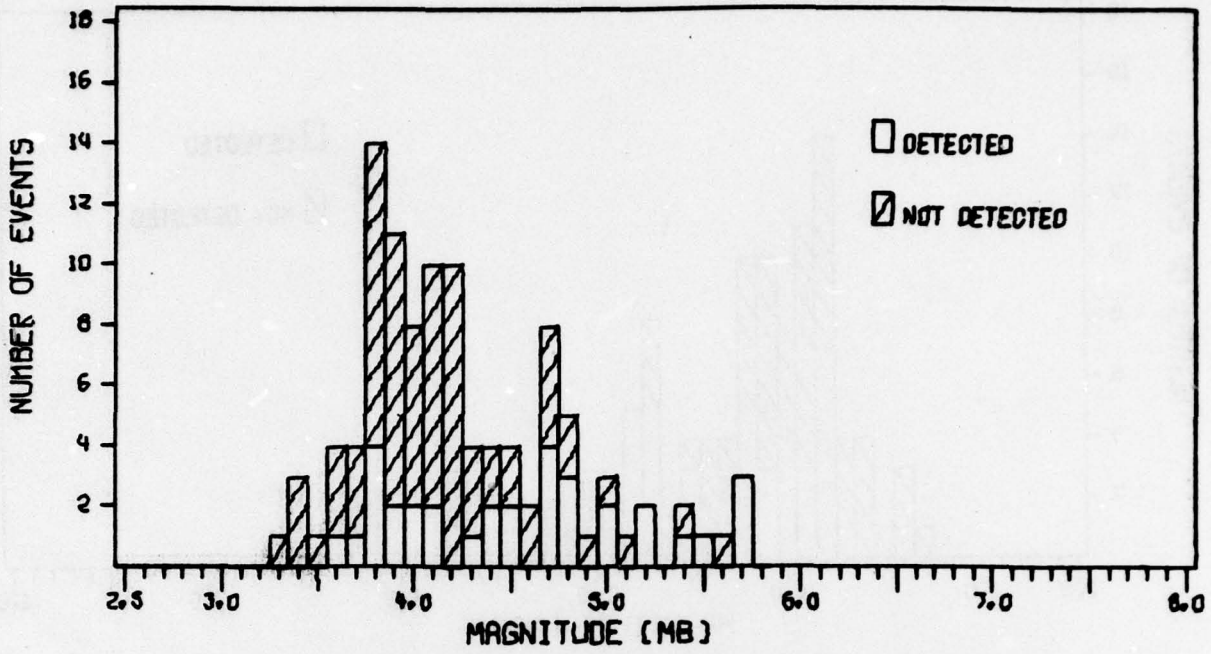

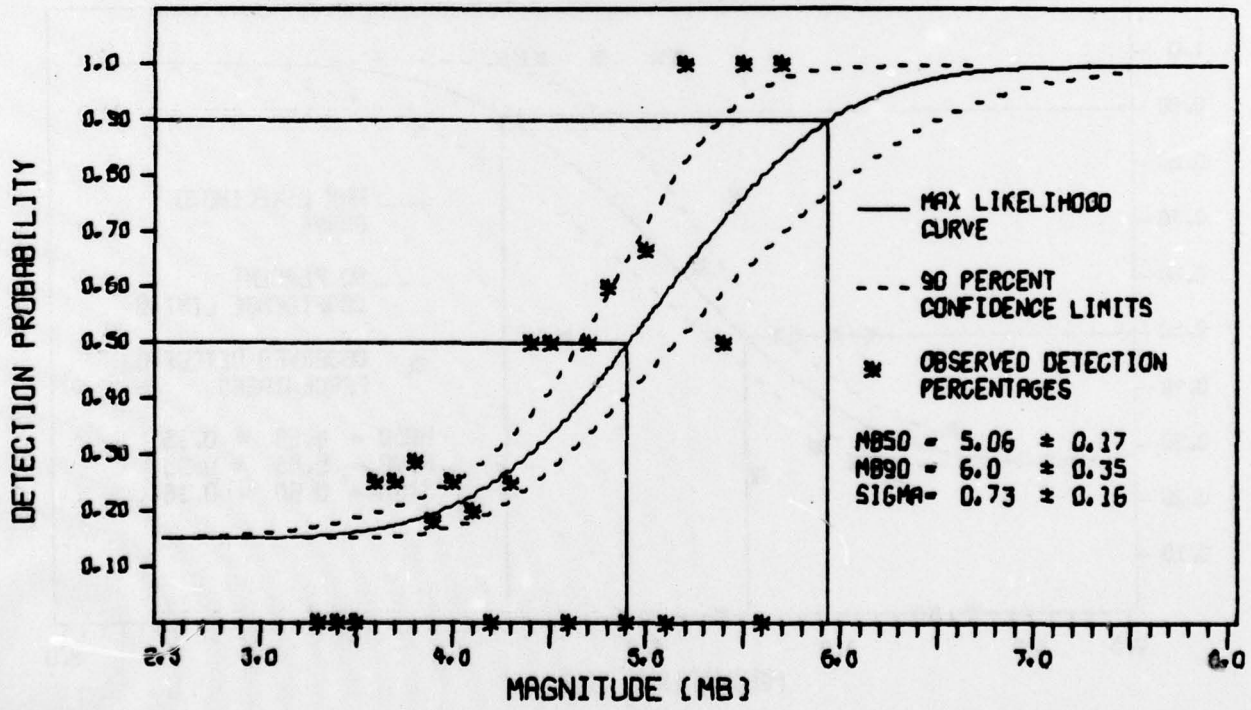

FIGURE IV-6

S WAVE ADAPTIVE FILTER DETECTIONS WITH
LIBERAL DETECTION CRITERIA

A substantial reduction in the P detection threshold has been accomplished at the expense of a false alarm rate of about 0.26. The 50% threshold at this alarm rate is about $m_b = 4.8$, down from 5.5 without the detector. The S detector shows no real improvement over the bandpass filter, even though its false alarm rate increased to 0.15.

In Figure IV-7 the epicenters of all those events in the data sample for which PDE data were available are plotted. The concentration of events near 44.5°N and 149.4°E suggests that those events share a common mechanism. That mechanism may be one which results in low bodywave magnitude for P waves at Guam, since all but two of these events were undetected with the P detector. Furthermore, those two events of $m_b = 5.7$ which were detected had long-period P wave magnitudes a full magnitude unit lower than that of the third $m_b = 5.7$ event in the sample, which was also detected but lay outside the region in question at the point marked 'A' in Figure IV-7.

Reliance on NORSAR detections to develop the data set has probably aggrevated this problem. It is plausible that all the events in the data set might have lobes in their P wave radiation patterns toward NORSAR but nulls near the direction of Guam. In that case no detector would give good results. A much more satisfactory data set would be one which depended for detections and short-period magnitudes on the PDE list or on short-period data taken at the same site as the long-period data.

B. MAGNITUDES

Despite these discouraging results, long-period bodywave magnitudes were calculated for all events detected using the criteria which led to the histogram of Figures IV-3 and IV-4. The standard expression for short-period bodywave magnitudes was used,

$$m_b = \log\left(\frac{A}{T}\right) + C$$

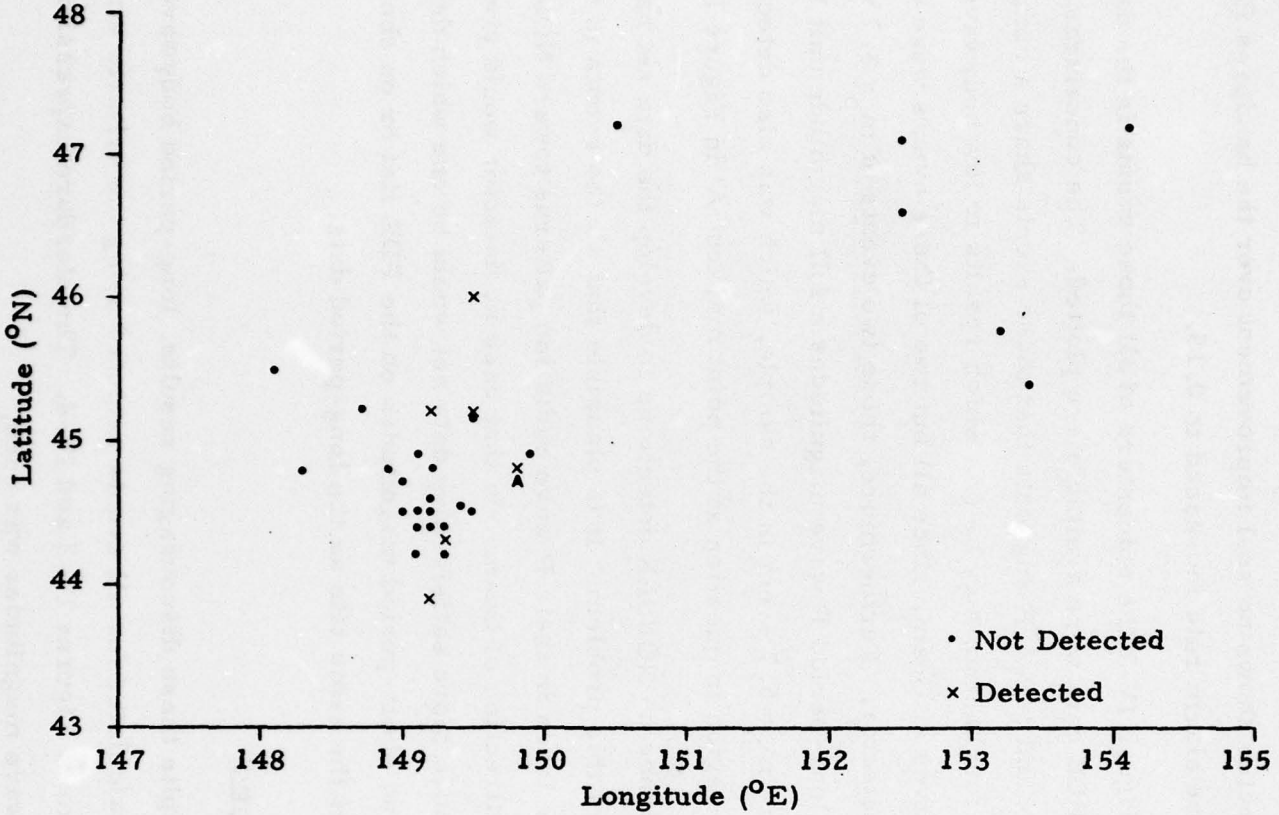

FIGURE IV-7

EPICENTERS FOR P WAVE DETECTIONS

where A is the peak amplitude of the vertical trace in millimicrons, T the period in seconds, and C a constant dependent on distance and tabulated by Vieth and Clawson (1972). These magnitudes are plotted versus short-period magnitude in Figure IV-8 for P detections.

If we accept the hypothesis that the events in the clustered near 44.5°N and 149.5°E are part of a swarm with low long-period amplitudes at Guam and eliminate them from Figure IV-8, only the two points at m_b = 2.9, m_b = 5.7 are dropped. The solid line is the best linear fit to the rest of the data. Considering the large number of false alarms implied by the detection curve of Figure IV-3, the correlation coefficient of 0.6 is probably reasonable. Since corner frequencies for earthquakes in this magnitude range are greater than the frequency at which short-period bodywave magnitudes are measured (Sax, 1975), both long-period and short-period magnitudes are measured on the flat part of the earthquake source spectrum. Consequently, the slope of the best fit to the data in Figure IV-8 should be 1.0, and the slope found there of 0.64 is not unreasonable considering the low quality of the data. Because of the large variance apparent in the m_b measurements of P waves, considerable more data are needed to establish their validity as discriminant measurements.

In contrast to the P detector results, all but one large event from those detected by the S wave detector lie within the earthquake swarm region near 44.5°N, 149.5°E, as shown in Figure IV-9. This is not unreasonable, since P and S waves do not have the same radiation pattern. Furthermore, all three magnitude 5.7 events have about the same long-period bodywave magnitude, and this magnitude is consistent with that of the smaller events, as shown in Figure IV-10, where m_b is plotted versus M_b for S waves. The slope of the best fit to the data is 0.53, consistent with that found for long-period P waves. Thus, the S wave data as well as the P wave data are consistent with the assumption that the particular data sample used here contributed to the poor results obtained. If this interpretation is correct, it is

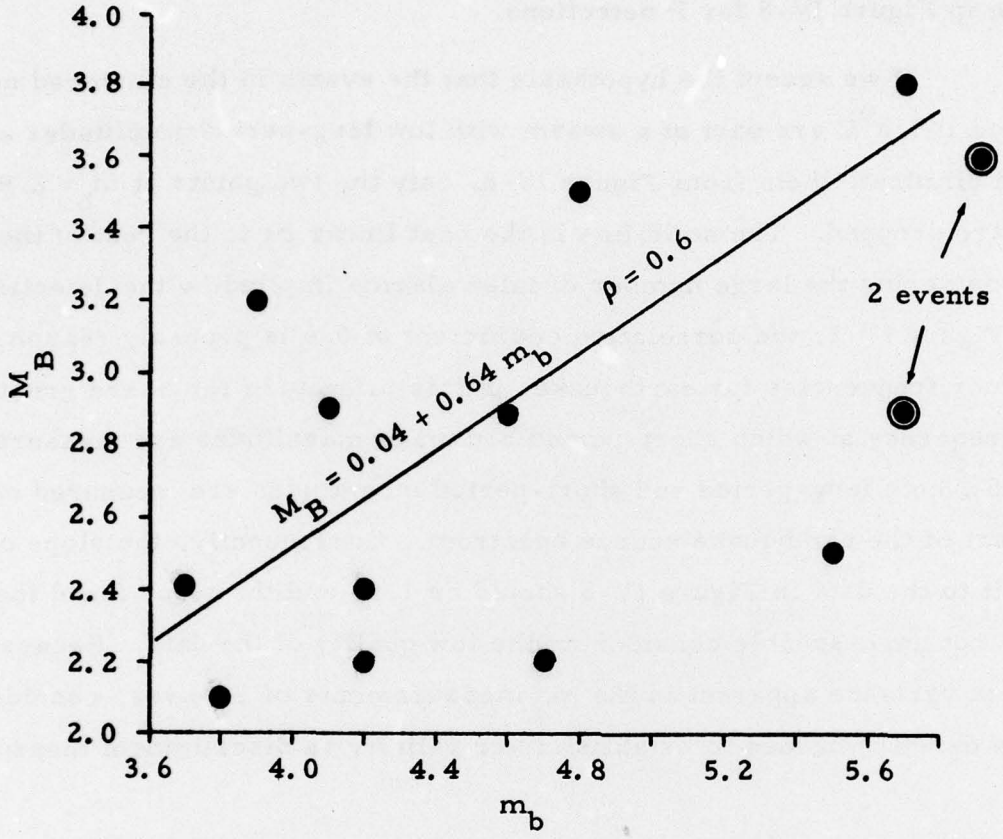

FIGURE IV-8

M_B VERSUS m_b FOR P WAVES

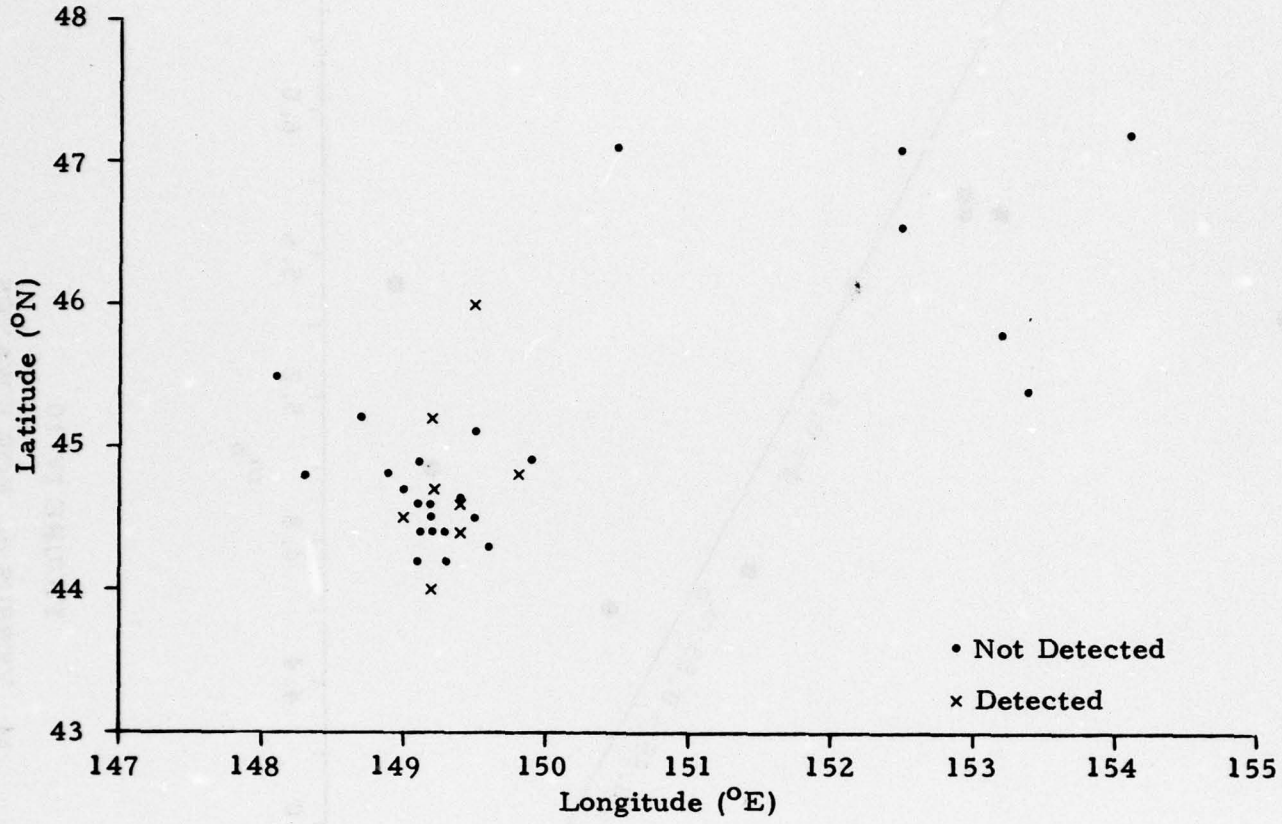

FIGURE IV-9

EPICENTERS FOR S WAVE DETECTIONS

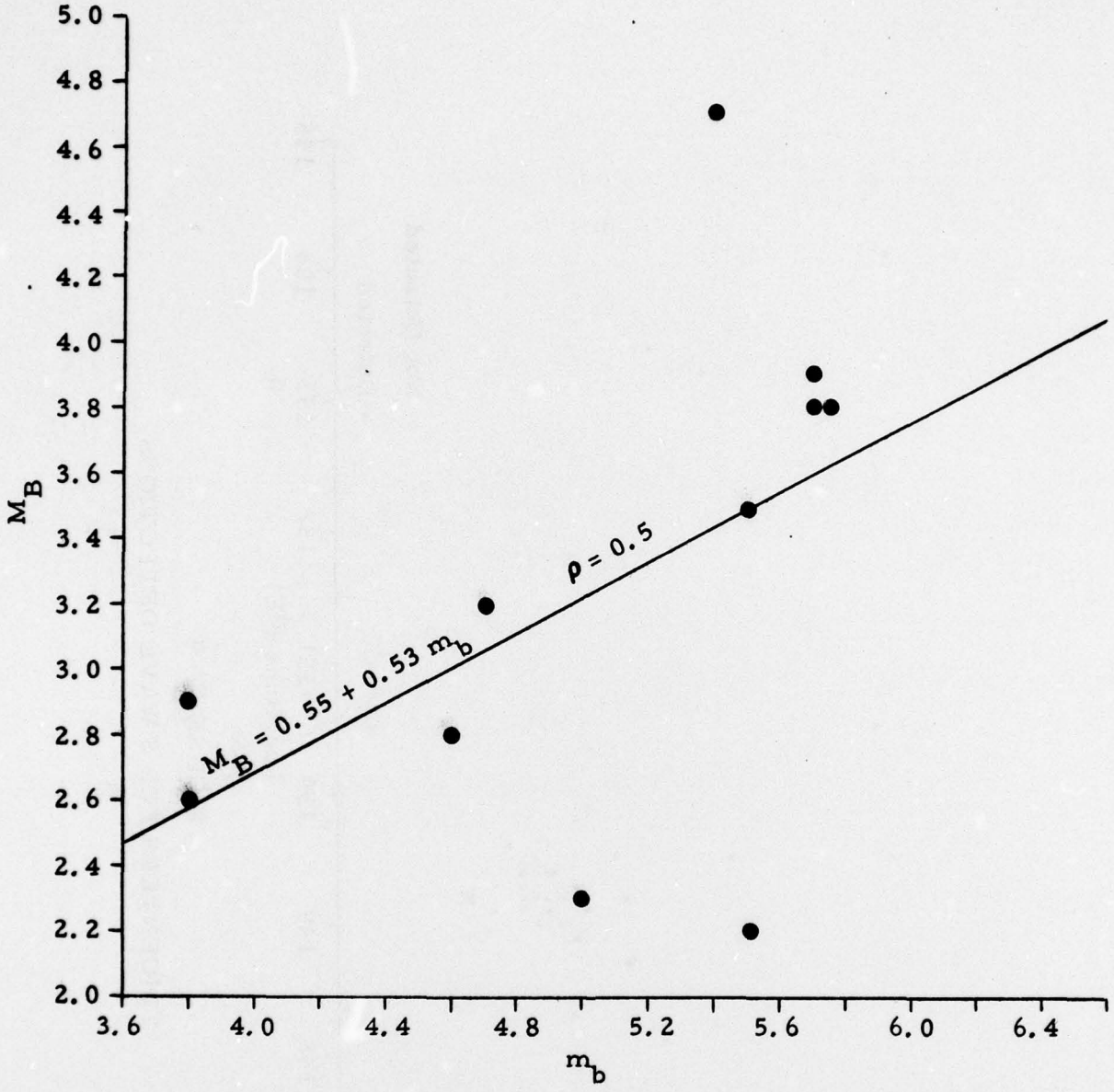

FIGURE IV-10

M_B VERSUS m_b FOR S WAVES

important to evaluate any future detector design on a data sample with wide enough spatial distribution that no bias due to radiation patterns is introduced.

The rather large values of sigma found on some of the fits to detection probabilities are probably due in part to this separation of the data into two populations. This results in wide variations in the long-period body-wave magnitude at a given short-period magnitude, and sigma is a measurement, in part, of this variation.

We may conclude from these results that the P detector at least is behaving qualitatively as it should, in that it passes signals while rejecting noise, but that the gain so achieved is not sufficient to make clear detections possible. The S detector seems to be behaving much worse, probably due to poor agreement between data and model, as evidenced by leakage of S energy onto the P detector traces.

SECTION V
CONCLUSIONS

Two conclusions can be drawn from this study. First, while the detectors studied here appear to be promising in terms of improvement in detection capability of long-period P waves, leakage of energy from phases which should be nulled by the detector probably leads to less than optimum performance. A model for the motion of P waves closer to the true particle motion should reduce this leakage and lower the detection threshold. Also, S wave particle motion should be investigated to explain the lack of positive results.

Second, there is evidence that part of the responsibility for the P detectors performance lies in apparent nulls in the radiation pattern peculiar to the data set used here. If this is the case, another data set should be used for any future evaluations. Some means may also be needed to correctly account for the effects of multiple radiation patterns on the detection capability of events from a given source region. Some consideration should be given to a joint measurement of long-period P wave and S wave bodywave magnitude which minimizes the effect of radiation patterns on detection and measurement of magnitude.

SECTION VI
REFERENCES

Kisslinger, C., E. R. Engdahl, G. Boucher, and R. Ganse, 1974; Semi-Annual Technical Report No. 2, Contract Number F44620-74-C-0015, Cooperative Institute for Research in Environmental Sciences, Boulder, Colorado.

Lane, S. S., 1976; Development of Three Signal Processing Techniques, Technical Report No. 6, Texas Instruments Report No. ALEX(01)-TR-76-06, AFTAC Contract Number F08606-76-C-0011, Texas Instruments Incorporated, Dallas, Texas.

Ringdal, F., 1974; Estimation of Seismic Detection Thresholds, Technical Report No. 2, Texas Instruments Report No. ALEX(01)-TR-74-02, AFTAC Contract Number F08606-74-C-0033, Texas Instruments Incorporated, Dallas, Texas.

Sax, R. L., 1975; Application of P Wave Spectral Measurements to Short-Period Discrimination, Technical Report No. 8, Texas Instruments Report No. ALEX(01)-TR-75-08, AFTAC Contract Number F08606-75-C-0029, Texas Instruments Incorporated, Dallas, Texas.

Strauss, A. C., and L. C. Weltman, 1977; Continuation of the Seismic Research Observatories Evaluation, Technical Report No. 2, Texas Instruments Report No. ALEX(01)-TR-77-02, AFTAC Contract Number F08606-77-C-0004, Texas Instruments Incorporated, Dallas, Texas.

Veith, K. V., and G. E. Clawson, 1972; Magnitude from Short-Period P Wave Data, Bulletin of the Seismological Society of America, 62, 435-452.